European Conference on Optical Communication (ECOC) 2022 © Optica Publishing Group 2022

# Partially Frozen MIMO Processing for Fast Polarisation Tracking

Akira Kawai(1), Masanori Nakamura(1), Minami Takahashi(1), Takayuki Kobayashi(1), Yutaka Miyamoto(1)

(1) NTT Network Innovation Laboratories, 1-1 Hikari-no-oka, Yokosuka, Kanagawa, Japan, akira.kawai.ku@hco.ntt.co.jp

**Abstract** *We proposed an adaptive equalisation scheme that has both fast polarisation tracking capability and transceiver IQ impairment tolerance based on partial freezing of the multiple-input multiple-output structure. Experimental results showed superior equalisation performance of the scheme to previous ones under polarisation fluctuations exceeding 11 Mrad/s. ©2022 The Author(s)*

## Introduction

Multiple-input multiple-output (MIMO) adaptive equalisation (AEQ) on a digital signal processor is a cornerstone technique for modern polarisation-division-multiplexed (PDM) coherent optical transmission systems [1]. Its ability to compensate for dynamic signal impairments like polarisation rotation or polarisation mode dispersion (PMD) is becoming more and more important as the trend of increasing symbol rates of transceivers continues, since high-symbol-rate signals are susceptible to such impairments.

Other than conventional 2×2 MIMO AEQ for PDM transmission, several types of AEQ can even compensate for IQ impairments within transceivers [1-5], e.g. IQ skew, amplitude/phase imbalance, or crosstalk, which are one of the main limiting factors of high-symbol-rate transmission [6]. Although IQ impairments can be calibrated before field deployment, adaptively equalising IQ impairments at the Rx-side is potentially important to maintain the signal quality since IQ impairments are slowly time-varying due to ageing or temperature dependence of the transceiver. Examples of such AEQs are 4×2 [2] and 8×2 MIMO AEQs [1]. By increasing the degrees of freedom (DOF) of the MIMO structure, they have a unique advantage in that they can deal with IQ impairments of the Rx (and the Tx too for the 8×2 MIMO AEQ). Although such AEQs suffer from increased computational complexity, techniques such as frequency-domain (FD) equalisation [7] can be used to reduce the complexity.

However, AEQs have a trade-off between the size of the internal DOF and the tracking speed because as the number of gradient descent-based AEQ taps increases, the trace of the covariance matrix of the corresponding input signals increases and limits the maximum step size of the AEQs [8]. So AEQs like 8×2 MIMO AEQ have degraded robustness to rapid fluctuations of the state of polarisation (SOP). As illustrated in Fig.1, extreme environmental factors such as lightning strikes can cause SOP fluctuations with the speed of over a few Mrad/s [9]. This can be an obstacle to the practical application of the transceiver-impairment-tolerant AEQs with increased DOF.

Here, we propose a method to improve the tracking speed of MIMO AEQs, namely, partial freezing. This method improves the tracking speed by temporary fixing the internal DOFs corresponding to the IQ distortion, taking advantage of the slow time variation of the IQ distortion in the transceiver. Experimental results show that under polarisation fluctuations of up to 11 Mrad/s, the proposed scheme outperforms conventional AEQs with little increase in computational complexity.

## Principle

The concept of the proposed partial freezing of MIMO AEQs is shown in Figure 2. In the proposed method, we decompose the MIMO structure into several matrix components, each of which represents SOP impairments and residual transceiver impairments. By freezing transceiver components, we can reduce the effective DOF and improve the tracking speed of the AEQ. In this work, we chose 8×2 MIMO AEQ as the main application of partial freezing for illustrative purposes. Also, we assumed FD AEQ [7] for the reduction of computational cost for the filtering.

The working principle and equalisation procedure are shown in the following. The 8×2 MIMO equalizer has a MIMO structure shown in

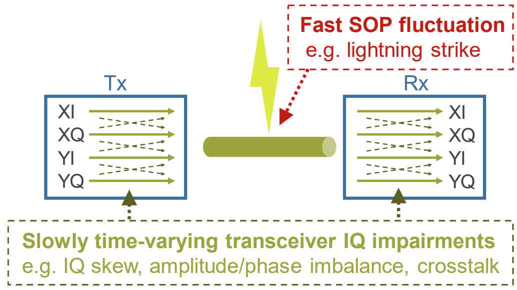


**Fig. 1:** Potential limiting factors of polarization-division-multiplexed optical transmission.

Fig.2, where $s_{\mathrm{x/y,in/out}}$ are input/output signals, $H_{8\times2,1}(\omega)$, $H_{8\times2,2}(\omega)$ are adaptively updatable 2×4 matrices

$$H_{8\times2,1}(\omega) := \begin{pmatrix} h_{\mathrm{xxo},1} & h_{\mathrm{xxc},1} & h_{\mathrm{xyo},1} & h_{\mathrm{xyc},1} \\ h_{\mathrm{yxo},1} & h_{\mathrm{yxc},1} & h_{\mathrm{yyo},1} & h_{\mathrm{yyc},1} \end{pmatrix},$$
$$H_{8\times2,2}(\omega) := \begin{pmatrix} h_{\mathrm{xxo},2} & h_{\mathrm{xxc},2} & h_{\mathrm{xyo},2} & h_{\mathrm{xyc},2} \\ h_{\mathrm{yxo},2} & h_{\mathrm{yxc},2} & h_{\mathrm{yyo},2} & h_{\mathrm{yyc},2} \end{pmatrix} \quad (1)$$

and $CD$ is the chromatic dispersion of the transmission line, $-\Delta\omega$ is the local oscillator (LO) frequency offset, and the asterisk represents complex conjugate (we use a different but equivalent definition of the input vector from that of previous research [1,7,10]). As shown in a previous work, the IQ impairment characteristics of transceivers can be obtained from the filter coefficients of the 8×2 MIMO equaliser [10]. One can show that

$$H_{8\times2,1}(\omega) = H'_{\mathrm{SOP}}(\omega)H'_{\mathrm{R}}(\omega),$$
$$H_{8\times2,2}(\omega) = H'^{*}_{\mathrm{T}}(-\omega)H'^{*}_{\mathrm{SOP}}(-\omega)\mathrm{H}'^{*}_{\mathrm{R}}(-\omega)P \quad (2)$$

where $\mathrm{H}'_{\mathrm{SOP}}(\omega)$ is a 2×2 matrix that represents the DOF of SOP, $\mathrm{H}'_{\mathrm{R}}(\omega)$ and $\mathrm{H}'_{\mathrm{T}}(\omega)$ are 4×2 and 2×2 matrix with four DOF that represents transceiver characteristics except for DOF of SOP and

$$P = \begin{pmatrix} 0 & 1 & 0 & 0 \\ 1 & 0 & 0 & 0 \\ 0 & 0 & 0 & 1 \\ 0 & 0 & 1 & 0 \end{pmatrix} \quad (3)$$

is a permutation matrix. We define each component of the characteristic matrices by

$$\mathrm{H}'_{\mathrm{SOP}}(\omega) := \begin{pmatrix} h_{\mathrm{xx}}(\omega) & h_{\mathrm{xy}}(\omega) \\ h_{\mathrm{yx}}(\omega) & h_{\mathrm{yy}}(\omega) \end{pmatrix},$$
$$\mathrm{H}'_{\mathrm{T}}(\omega) := \begin{pmatrix} h'_{\mathrm{T}11}(\omega) & h'_{\mathrm{T}12}(\omega) \\ h'_{\mathrm{T}21}(\omega) & h'_{\mathrm{T}22}(\omega) \end{pmatrix}, \quad (4)$$
$$\mathrm{H}'_{\mathrm{R}}(\omega) := \begin{pmatrix} 1 & h'_{\mathrm{R}11}(\omega) & 0 & h'_{\mathrm{R}12}(\omega) \\ 0 & h'_{\mathrm{R}21}(\omega) & 1 & h'_{\mathrm{R}22}(\omega) \end{pmatrix}.$$

Then, one can also show each component can be obtained from the coefficients of the 8×2 MIMO equaliser:

$$H'_{\mathrm{SOP}} = \begin{pmatrix} h_{\mathrm{xxo},1} & h_{\mathrm{xyo},1} \\ h_{\mathrm{yxo},1} & h_{\mathrm{yyo},1} \end{pmatrix},$$
$$H'_{\mathrm{T}} = \begin{pmatrix} h^{*}_{\mathrm{xxc},2}(-\omega) & h^{*}_{\mathrm{xyc},2}(-\omega) \\ h^{*}_{\mathrm{yxc},2}(-\omega) & h^{*}_{\mathrm{yyc},2}(-\omega) \end{pmatrix} H'^{-1}_{\mathrm{SOP}}, \quad (5)$$
$$\begin{pmatrix} h'_{\mathrm{R}11} & h'_{\mathrm{R}12} \\ h'_{\mathrm{R}21} & h'_{\mathrm{R}22} \end{pmatrix} = H'^{-1}_{\mathrm{SOP}} \begin{pmatrix} h_{\mathrm{xxc},1} & h_{\mathrm{xyc},1} \\ h_{\mathrm{yxc},1} & h_{\mathrm{yyc},1} \end{pmatrix}.$$

Therefore, once the coefficients of the 8×2 MIMO AEQ are obtained, we can seamlessly switch to the decomposed description illustrated in the lower part of Fig. 2, and continue the equalisation by updating only $H'_{\mathrm{SOP}}$ and keep $H'_{\mathrm{T}}(\omega)$ and $H'_{\mathrm{R}}(\omega)$ frozen. Also, we can switch back to the normal 8×2 description when the IQ impairment characteristics change.

Among possible update algorithms for $H'_{\mathrm{SOP}}$, we adopt the gradient descent method. In this configuration, the update formula is $H'_{\mathrm{SOP}}(m+1) = H'_{\mathrm{SOP}}(m) + \mu(\boldsymbol{e}\exp(-\mathrm{i}\Delta\omega t)\,\boldsymbol{s}_1^{\dagger} + H'^{\dagger}_{\mathrm{T}}(\omega)\boldsymbol{e}\exp(\mathrm{i}\Delta\omega t)\,\boldsymbol{s}_2^{\dagger})$, where $m$ is a time index, $\mu$ is a step size, $\boldsymbol{e}$ is an error vector obtained by subtracting demodulated signals from hard-decided symbols, and $\boldsymbol{s_1} = H'_{\mathrm{R}}(\omega)CD^{-1}\boldsymbol{s_{out}}$, $\boldsymbol{s_2} = H'^{*}_{\mathrm{R}}(-\omega)\mathrm{CD}\boldsymbol{s_{out}}$ are vectors that can be obtained in the process of the equalisation.

As for the computational complexity, partial freezing of 8×2 MIMO AEQ gives little increase in complexity. For example, the number of multiplication operations required for the matrix computations during equalisation of one frequency component using a partially frozen 8×2 MIMO AEQ is 20 and that during update is 12, while the normal one requires 16 during both equalisation and update. Also, since the fast Fourier transform (FFT) accounts for the majority of the total complexity of the FD AEQ, changes in the complexity of the filtering itself have little effect on the total here.

Note that the concept of partial freezing can be applied to other MIMO structures. For example, to apply it to the 4×2 MIMO AEQ, one can derive the entire equalisation procedure by simply ignoring the lower branch of the 8×2 MIMO structure illustrated in Fig.2.

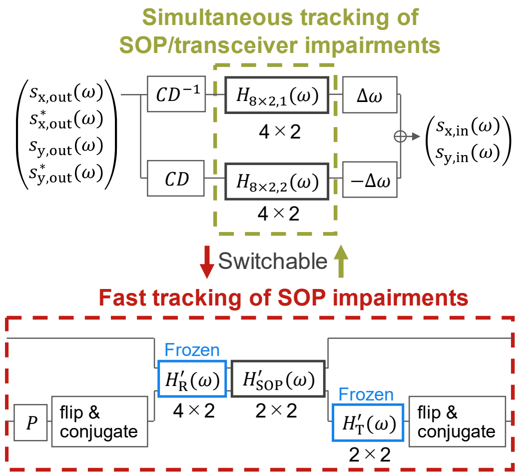


**Fig. 2:** A conceptual illustration of partial freezing of MIMO AEQ, here represented by an 8×2 MIMO AEQ.

## Experiments

We conducted proof-of-principle experiments with 128 Gbaud high-speed signals and rapid SOP fluctuations emulated by a polarisation scrambler. Fig. 3 describes the schematic of the setup. A light from a low-phase-noise laser at 193.755 THz was modulated by a 35 GHz-bandwidth PDM IQ modulator. Electrical modulation signals were generated by an arbitrary waveform generator (AWG) with four 65 GHz-bandwidth digital-to-analogue converters

(DAC) driven at 128 Gsample/s. The modulation format was quadrature phase shift keying (QPSK) randomly generated by the Marsenne Twister. The frame length of the signal was 65536. The signal light was amplified by an erbium-doped fibre amplifier (EDFA), and spectrally shaped by an optical equalisation (OEQ) [11]. The SOP of the signal lights was modulated by a high-speed polarisation scrambler (PS). Our PS (MPC-203, General Photonics) scrambled the SOP at variable maximum speeds up to 11.01 Mrad/s. Before and after the PS, 10- and 40-m-long polarisation maintaining fibres (PMF) were placed to confirm the existence of PMD does not affect the effectiveness of our method. After amplification by another EDFA and optical filtering of noise outside the modulation bandwidth by an optical band-pass filter (OBPF), signals were mixed with a light from an LO and detected by a coherent receiver at 256 Gsample/s. To see the IQ impairment tolerance of the AEQs, 3 ps IQ skews were imposed on the x-polarisation signals in both AWG and Rx-side digital signal processing (DSP), along with intrinsic IQ impairments such as IQ skews arising from variations in coaxial cable lengths or electrical crosstalk.

At the Rx-side DSP, the signal was demodulated using 50% overlap cut FD MIMO AEQ, coarse carrier phase recovery (CPR) with a 2nd-order digital phase-looked loop, and a fine CPR with a blind phase search algorithm [12]. To run the partially frozen (PF) 8×2 MIMO AEQ, $H'_{\mathrm{T}}(\omega)$ and $H'_{\mathrm{R}}(\omega)$ were obtained before the demodulation and averaged using signals of 50 frames. The signal-to-noise ratio (SNR) of the signal was evaluated after the demodulation by varying the step size and the FFT size. For the SNR evaluation procedure, we calculated the SNR of consecutive 10 frames and picked up the worst one as the SNR of the signal, as the SOP rate of change was time-variant.

The experimental results are shown in Fig. 4. First, to see the maximum performance of the proposed AEQ when the SOP rapidly fluctuates, we modulated the SOP at the maximum rate of change of 11.01 Mrad/s and demodulated them with PF 8×2, 8×2, 4×2 and 2×2 MIMO AEQs. We

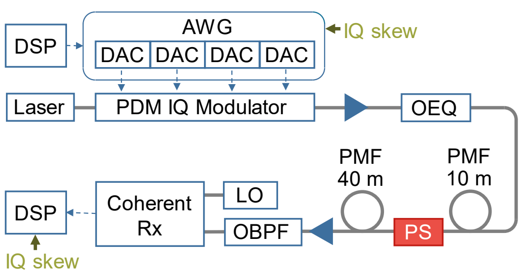


**Fig. 3:** Schematic of the experimental setup.

varied the FFT size of the FD AEQ, and for each FFT size, the step size was optimised. The results are shown in Fig. 4(a), where the PF 8×2 MIMO AEQ shows the optimal performance at an FFT size of 1024 (corresponding to a 4 ns time window) since it can compensate for spectrally fine transceiver IQ impairments with a larger step size than a normal 8×2 MIMO AEQ.

Next, we varied the step size while fixing the FFT size to 1024, and saw the SNR difference between different AEQs. The results are shown in Fig. 4(b). The PF AEQ worked with about a two-times-larger step size than the normal one before becoming unstable, which demonstrated a 4.4 dB SNR advantage over normal one.

## Conclusion

In this work, we proposed the partial freezing of a MIMO structure that enables adaptive equalising of the signal which is simultaneously robust to fast SOP fluctuations and has tolerance to transceiver IQ impairments. The concept is based on the fact that transceiver-impairment-tolerant MIMO structures can be decomposed to DOF that represents the SOP and the transceiver, and freezing the latter DOF contributes to increased polarisation tracking speed. We tested the scheme with SOP fluctuations of over 11 Mrad/s and showed the method has a 4.4 dB SNR advantage over the normal 8×2 MIMO AEQ.

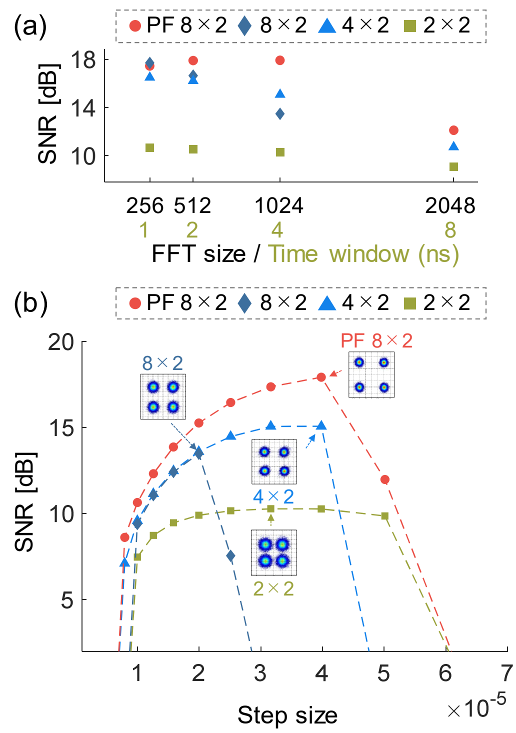


**Fig. 4:** (a) Evaluated SNR of the signals whose SOP is fluctuated at the speed up to 11.01 Mrad/s (step size optimized). Corresponding lengths of time windows are also shown. (b) Step size and the SNR at FFT size of 1024.

## References

[1] T. Kobayashi, M. Nakamura, F. Hamaoka, M. Nagatani, H. Wakita, H. Yamazaki, T. Umeki, H. Nosaka, and Y. Miyamoto, "35-Tb/s C-band Transmission over 800 km Employing 1-Tb/s PS-64QAM signals enhanced by Complex 8 × 2 MIMO Equalizer," in Proceedings of Optical Fiber Communication Conference 2019, San Diego, United States, 2019, paper Th4B.2, DOI: 10.1364/OFC.2019.Th4B.2

[2] R. Rios-Müller, J. Renaudier, and G. Charlet, "Blind Receiver Skew Compensation and Estimation for Long-Haul Non-Dispersion Managed Systems Using Adaptive Equalizer," Journal of Lightwave Technology, Vol. 33, no. 7, pp. 1315-1318, 2015, DOI: 10.1109/JLT.2014.2377582

[3] C. R. S. Fludger and T. Kupfer, "Transmitter Impairment Mitigation and Monitoring for High Baud-Rate, High Order Modulation Systems," in Proceedings of 42nd European Conference on Optical Communication, Düsseldorf, Germany, 2016, paper Tu.2.A.2.

[4] M. Arikawa and K. Hayashi, "Adaptive equalization of transmitter and receiver IQ skew by multi-layer linear and widely linear filters with deep unfolding," Optics Express, vol. 28, pp. 23478-23494, 2020, DOI: 10.1364/OE.395361

[5] M. Sato, M. Arikawa, H. Noguchi, J. Matsui, J. Abe, and E. L. T. De Gabory, "Mitigation of Transmitter Impairment with 4×2 WL MIMO Equalizer Embedding Preliminary CPR," in Proceedings of Optical Fiber Communication Conference 2022, San Diego, United States, 2022, paper M1H.5, DOI: 10.1364/OFC.2022.M1H.5

[6] X. Chen, J. Cho, A. Adamiecki, and P. Winzer, "16384-QAM transmission at 10 GBd over 25-km SSMF using polarization-multiplexed probabilistic constellation shaping." in Proceedings of 45th European Conference on Optical Communication, Dublin, United Kingdom, 2019, paper PD3.3, DOI: 10.1049/cp.2019.1030

[7] M. Nakamura, T. Kobayashi, F. Hamaoka, and Y. Miyamoto, "High Information Rate of 128-GBaud 1.8-Tb/s and 64-GBaud 1.03-Tb/s Signal Generation and Detection Using Frequency-Domain 8×2 MIMO Equalization," in Proceedings of Optical Fiber Communication Conference 2022, San Diego, United States, 2022, paper M3H.1, DOI: 10.1364/OFC.2022.M3H.1

[8] P. S. R. Diniz, *Adaptive filtering,* 4th ed. Berlin, Germany: Springer, 2012, DOI: 10.1007/978-1-4614-4106-9

[9] D. Charlton, S. Clarke, D. Doucet, M. O'Sullivan, D. L. Peterson, D. Wilson, G. Wellbrock, and M. Bélanger, "Field measurements of SOP transients in OPGW, with time and location correlation to lightning strikes," Optics Express, vol. 25, pp. 9689-9696, 2017, DOI: 10.1364/OE.25.009689

[10] A. Kawai, M. Nakamura, T. Kobayashi, and Y. Miyamoto, "4-Dimensional IQ Characteristic Estimation for Polarization-multiplexed Coherent Transceivers," in Proceedings of Optical Fiber Communication Conference 2022, San Diego, United States, 2022, paper M1H.2, DOI: 10.1364/OFC.2022.M1H.2

[11] A. Matsushita, M. Nakamura, K. Horikoshi, S. Okamoto, F. Hamaoka, and Y. Kisaka, "64-GBd PDM-256QAM and 92-GBd PDM-64QAM Signal Generation using Precise-Digital-Calibration aided by Optical-Equalization," in Proceedings of Optical Fiber Communication Conference 2022, San Diego, United States, 2022, paper W4B.2, DOI: 10.1364/OFC.2019.W4B.2

[12] T. Pfau, S. Hoffmann, and R. Noé, "Hardware-Efficient Coherent Digital Receiver Concept With Feedforward Carrier Recovery for $M$-QAM Constellations," Journal of Lightwave Technology, Vol. 27, no. 8, pp. 989-999, 2009, DOI: 10.1109/JLT.2008.2015511